Improvement of the SWAT model for event-based flood forecasting on a sub-daily time scale

Dan Yu[1], Ping Xie[1,2], Xiaohua Dong[3,4], Xiaonong Hu[5], Ji Liu[3,4], Yinghai Li[3,4], Tao Peng[3,4], Haibo Ma[3,4], Kai Wang[6], Shijin Xu[6]

[1]State Key Laboratory of Water Resources and Hydropower Engineering Science, Wuhan University, Wuhan, 430072, China
[2]Collaborative Innovation Center for Territorial Sovereignty and Maritime Rights, Wuhan, 430072, China
[3]College of Hydraulic & Environmental Engineering, China Three Gorges University, Yichang, 443002, China
[4]Hubei Provincial Collaborative Innovation Center for Water Security, Wuhan, 430070, China
[5]Institute of Groundwater and Earth Sciences, Jinan University, Guangzhou 510632, China
[6]Hydrologic Bureau of Huaihe River Commission, Bengbu, 233001, China

Correspondence to: Ping Xie (pxie@whu.edu.cn)

Abstract. Flooding represents one of the most severe natural disasters threatening the development of human society. Flood forecasting systems imbedded with hydrological models are some of the most important non-engineering measures for flood defense. The Soil and Water Assessment Tool (SWAT) is a well-designed hydrological model that is widely applied for runoff and water quality modeling. The original SWAT model is a long-term yield model. However, a daily simulation time step and continuous time marching limit the application of the SWAT model for detailed, event-based flood forecasting. In addition, SWAT uses a basin level parameter that is fixed for the whole catchment to parameterize the Unit Hydrograph (UH), thereby ignoring the spatial heterogeneity among the sub-basins when adjusting the shape of the UHs. This paper developed a method to perform event-based flood forecasting on a sub-daily time scale based on SWAT2005 and simultaneously improved the UH method used in the original SWAT model. First, model programs for surface runoff and water routing were modified for a sub-daily time scale. Subsequently, the entire loop structure was broken into discrete flood events in order to obtain a SWAT-EVENT model in which antecedent soil moisture and antecedent reach storage could be obtained from daily simulations of the original SWAT model. Finally, the original lumped UH parameter were refined into distributed parameters to reflect the spatial variability of the studied area. The modified SWAT-EVENT model was used in the Wangjiaba catchment located in the upper reaches of the Huaihe River in China. Daily calibration and validation procedures were first performed for the SWAT model with long-term flow data from 1990 to 2010, after which sub-daily ($\Delta t = 2$ h) calibration and validation in the SWAT-EVENT model were conducted with 24 flood events originating primarily during the flood seasons within the same time span. Daily simulation results demonstrated good model performances with Nash-Sutcliffe efficiency coefficient (E_{NS}) values of 0.80 and 0.83 for the calibration and the validation, respectively. Event-based flood simulation results indicated reliable performances, with E_{NS} values varying from 0.68 to 0.93. The SWAT-EVENT model, compared to the SWAT model, particularly improved the simulation accuracies of the flood peaks. Furthermore, the SWAT-EVENT model results of the two

UH parameterization methods indicated that the use of the distributed parameters resulted in a more reasonable UH characterization and better model fit compared to the lumped UH parameter.
Keywords: SWAT model; Event-based flood forecasting; Antecedent conditions; Unit Hydrograph

1 Introduction

A flood represents one of the most severe natural disasters in the world. It has been reported that nearly 40 % of losses originating from natural catastrophes are caused by floods (Adams Iii and Pagano, 2016). Numerous measures have been designed to defend against the threats of flooding. Of the many non-engineering measures, flood forecasting is one of the most important. A complete flood forecasting system consists of many different functional components, the most significant of which is the hydrological model.

Numerous hydrological models have been developed since their first appearance. According to the spatial discretization method, these existing hydrological models can be divided into two categories: lumped models and distributed (semi-distributed) models (Maidment, 1994). Although lumped models are commonly accepted for research and associated applications, they are not applicable to large catchments since they do not account for the heterogeneity of the catchments (Yao et al., 1998). Meanwhile, distributed (semi-distributed) models subdivide the entire catchment into a number of smaller heterogeneous sub-units with dissimilar attributes. A large number of distributed or semi-distributed hydrological models have been applied in flood forecasting (BEVEN and KIRKBY, 1979;Singh, 1997;Xiong and Guo, 2004;Mendes and Maia, 2017;Hapuarachchi et al., 2011).

The Soil and Water Assessment Tool (SWAT) model was developed by the United States Department of Agriculture (USDA) in 1994 and represents a typical semi-distributed hydrological model that can simulate long-term surface and subsurface discharge, sediment deposition, nutrient transport and transformation processes under varying land uses, soil types and management conditions. To spatially characterize the inhomogeneity, the SWAT model delineates a catchment into a number of sub-basins, which were subsequently divided into Hydrologic Response Units (HRUs). In the SWAT model, HURs are basic simulation units of the land phase of the hydrological cycle that controls the total yield of streamflow, sediment, pesticide and nutrient to the main channel in corresponding sub-basin. Afterwards the routing phase converges the land phase results to the watershed outlet through the channel network. The SWAT model has been widely applied throughout the world (Gassman et al., 2010), with corresponding research involving runoff simulation, non-point source pollution, model parameters, hydrological responses to changed scenarios and so on.

SWAT is a continuous (i.e., long-term) model (Kiniry et al., 2005) with a limited applicability toward simulating instantaneous hydrologic responses. Therefore, Jeong et al. (2010) extended the capability of SWAT to simulate operational sub-daily or even sub-hourly hydrological processes, the modifications of which primarily focused on the model algorithms to enable the SWAT model to operate at a finer time scale with a continuous modeling loop. According to flood forecasting programs and technology in China (MWR, 2009), rainfall and discharge observations at a sub-daily time scale are usually only collected during flood periods, while daily data are measured otherwise. Hydrological models are usually applied at different time scales (i.e., a daily time scale for continuous simulations and a sub-daily time scale for event-based flood forecasting) according to the availability of observed rainfall and discharge data (Yao et al., 2014). Hence, a major constraint for the application of the SWAT model as modified by Jeong et al. (2010) is the conflict between a continuous simulation loop and the discontinuous observed sub-daily data in China.

To capture the sophisticated characteristics of flood events at a sub-daily time scale, a refinement of the spatial representation within the SWAT model is necessary. A dimensionless Unit Hydrograph (UH), which was distributed as a triangular shape and embedded within an sub-daily overland flow routing process in the SWAT model, was applied to relate hydrologic responses to specific catchment characteristics, such as the dimensions of the main stream and basin area, through applications of Geographic Information System (GIS) or Remote Sensing (RS) software (Jena and Tiwari, 2006). Due to the spatial discretization in the SWAT model, the model parameters are grouped into three levels: (1) basin level parameters are fixed for the whole catchment; (2) sub-basin level parameters are varied with sub-basins; (3) HRU level parameters are distributed in different HRUs. By default, the UH-specific parameters in the SWAT model are programmed on the basin level, which means that no spatial variation within a catchment is possible when adjusting the shape of the UH in each sub-basin. Given the spatial heterogeneity of the catchment, the application of this basin level adjustment parameter seems to be rather unconvincing. Moreover, because a great deal of research has primarily focused on daily, monthly or yearly simulations using the SWAT model, little effort has actually been provided toward demonstrating the usage of the UH method in the SWAT model.

This study developed a method to perform event-based flood forecasting on a sub-daily time scale based on the SWAT model and simultaneously improved the UH method used in the original SWAT model in the upper reaches of the Huaihe River in China. SWAT is an open-source code model, which makes it possible to produce such a modification. The SWAT2005 version has an existing auto-calibration module and such integrated design of model simulation and auto-calibration is easily manageable and modified since there is no need to couple external optimization algorithms.

2 Study area and data

2.1 Study area

The Huaihe River basin (30°55'–36 °36' N, 111°55'–121°25' E) is situated in the eastern part of China. The Wangjiaba (WJB) catchment is situated within the upper reaches of the Huaihe River basin and was chosen as the study area for this paper (see Fig. 1). The WJB catchment has a drainage area of 30630 km^2, wherein the long channel reaches from the source region to the WJB outlet. The southwestern upstream catchment is characterized as a mountain range with a maximum elevation of 1110 m above sea level. The central and eastern downstream regions are dominated by plains. The study catchment is a subtropical zone with an annual average temperature of 15 °C. The long-term average annual rainfall varies from 800 mm in the north to 1200 mm in the south. Since the catchment is dominated by a monsoon climate, approximately 60 % of the annual rainfall is received during the flood season ranging from mid-May to mid-October. Severe rainfall events within the study area typically transpire during the summer, frequently resulting in severe floods (Zhao et al., 2011).

2.2 Model dataset

To construct and execute the SWAT model, a Digital Elevation Model (DEM), together with land use and soil type data, is required. Climate data, including that of rainfall, temperature, wind speed, etc., are also used. Table 1 lists the model data used in this study.

The DEM data in this study were downloaded from the website of the U.S. Geological Survey (USGS) with a spatial resolution of 90 m. Since there is no specific instruction to subdivide the catchment, the threshold sub-basin size was decided by the model developer, depending on the computational time and the size of the catchment (Romanowicz et al., 2005). Consequently, the study catchment was divided into 21 sub-basins according to the given threshold of 844.64 km^2, as shown in Fig. 1. The geographic features of all the sub-basins are displayed in Table 2.

A land use map was produced from the Global Land Cover 2000 (GLC2000) data product with a grid size of 1 km (Bartholomé and Belward, 2005). Six categories of land use were identified for this catchment, as are shown in Fig. 2 (a): agricultural land (80.51 %), forest-deciduous (6.76 %), forest-evergreen (2.26 %), range-brush (1.09 %), range-grasses (8.09 %) and water (1.29 %).

Soil data were obtained from the Harmonized World Soil Database (HWSD) with a spatial resolution of 30 arc-seconds. The HWSD also provides an attributed database that contains the physico-chemical characteristics of soil data worldwide (Nachtergaele et al., 2012). Since the built-in soil database within the SWAT model does not cover the study area, additional soil parameters were calculated using the method proposed by Jiang et al. (2014). Fig. 2 (b) exhibits the distribution of soil types in the study area according to the FAO-90 soil classification. Consequently, Eutric Planosols and Cumulic Anthrosols are the two main soil types with area percentages of 24.71 % and 19.95 %, respectively.

The SWAT model has developed a weather generator (WXGEN) to fill the missing climate data by the use of monthly statistics. Relative humidity, wind speed, solar radiation and the minimum and maximum air temperatures were obtained from the Climate Forecast System Reanalysis (CFSR), which was designed based on the forecast system of the National Centers for Atmospheric Prediction (NCEP) to provide estimation for a set of climate variability from 1979 to the present day. There were 30 weather stations included in the study catchment.

A dense rain gauge network consisting of 138 gauges is distributed throughout the study area, as illustrated in Fig. 1. Thiessen average rainfall was calculated to incorporate spatially variable rainfall in each sub-basin. Daily observed rainfall data were retrieved from 1991 to 2010 with coverage during the entire year, while sub-daily ($\Delta t = 2$ h) rainfall data are only available for flood periods from May to September during the years 1991 and 2010.

3 Methodologies

3.1 Development of a sub-daily event-based SWAT model

The original SWAT model was designed for continuous simulations using a daily time step. The SWAT model operates most effectively during the prediction of long-term catchment responses to land cover changes or soil management practices (Jeong et al., 2011). When faced with flood forecasting issues, a finer time scale is required to realistically capture the instantaneous changes representative of flood processes. Within the flood forecasting program and technology of China, discharges are observed daily during the dry seasons, which is intensified to sub-daily during flooding seasons in order to depict the details of flooding hydrographs and provide timely flood warnings (MWR, 2009).

Therefore, the original daily simulation-based SWAT model first needs to be modified in order to perform sub-daily simulations. In a previous study, the sub-daily and even the sub-hourly modeling capacities of the SWAT model have been developed to allow flow simulations with any time step less than a day (Jeong et al., 2010). In the original SWAT model, the surface runoff lag was estimated by a first order lag equation, which was represented by a function of the concentration time and the lag parameter. However, this lag equation was implicitly fixed with daily time interval. Jeong et al. (2010) then introduced the simulation time interval into the lag equation to lag a fraction of the surface runoff at the end of each time step. In addition, channel and impoundment routings were also estimated at operational time interval while other processes such as base flow and evapotranspiration were calculated by equally dividing the daily results over the time steps. In this study, the modifications from daily modeling to sub-daily modeling followed the methods proposed by Jeong et al. (2010). Second, the modified sub-daily SWAT model must be applied in such a manner to achieve the simulation of individual flooding events rather than to simulate in a continuous way, as performed in the original SWAT model. Event-based flood modeling is necessary for these reasons: (1) to enable the modelers to acknowledge the detailed information of up-coming floods and (2) to potentially conduct flood forecasting within a watershed without possessing continuously recorded hydrologic data at short time step. To enable the SWAT model to simulate flood events, the original source codes were modified and compiled into a new version known as SWAT-EVENT. In the source code of SWAT2005, the subroutine "simulate" contains the loops governing the hydrological processes following the temporal marching during the entire simulation period. Here, the continuous yearly loop was set into several flood events, meanwhile, the continuous daily loop was broken into flood periods according to the specific starting and ending dates.

However, the event-based modeling requires a separate method to derive the antecedent conditions of model states. The combination of daily continuous modeling and sub-daily event-based modeling was used in this study (Fig. 3). A continuous daily rainfall sequence was imported into the original SWAT model to independently perform long-term daily simulations. In the SWAT model, there are another two subroutines "varinit" and "rchinit" initializing the daily simulation variables for the land phase of the hydrologic cycle and the channel routing, respectively. In the SWAT-EVENT model, condition judgments were added into those two initialization subroutines. That is, when the simulation process is at the beginning of a given flood event, antecedent soil moisture and antecedent reach storage are set equal to the respective values extracted from the long-term daily simulations of the original SWAT model; otherwise, they should be updated by the SWAT-EVENT model simulation states of the previous day.

3.2 Application of Unit Hydrographs with distributed parameters

The dimensionless UH method employed in the SWAT model exhibits a triangular shape (SCS, 1972), as shown in Fig. 4, wherein the time t (h) represents the X-axis, and the ratio of the discharge to peak discharge represents the Y-axis. This UH is defined as follows:

$$q_{\mathrm{uh}} = \frac{t}{t_{\mathrm{p}}} \quad \text{if } t \le t_{\mathrm{p}}$$
$$q_{\mathrm{uh}} = \frac{t_{\mathrm{b}} - t}{t_{\mathrm{b}} - t_{\mathrm{p}}} \quad \text{if } t > t_{\mathrm{p}} \tag{1}$$

where q_{uh} is the unit discharge at time t, t_{p} is the time to the peak (h), and t_{b} is the time base (h). Then, the dimensionless UH is expressed by dividing by the area enclosed by the triangle (Jeong et al., 2010). There are two time factors that determine the shape of the triangular UH, and they are defined by the following equations:

$$t_{\mathrm{b}} = 0.5 + 0.6 \cdot t_{\mathrm{c}} + t_{\mathrm{adj}} \tag{2}$$

$$t_{\mathrm{p}} = 0.375 \cdot t_{\mathrm{b}} \tag{3}$$

where t_{c} is the concentration time for the sub-basin (h), and t_{adj} is a shape adjustment factor for the UH (h) (Neitsch et al., 2011).

The time of concentration t_{c} can be calculated based upon the geographic characteristics of the sub-basin considered, for which t_{c} is denoted by the accumulation of the overland flow time t_{ov} (h) and the channel flow time t_{ch} (h):

$$t_{\mathrm{c}} = t_{\mathrm{ov}} + t_{\mathrm{ch}} \tag{4}$$

$$t_{\mathrm{ov}} = \frac{L_{\mathrm{slp}}^{0.6} \cdot n^{0.6}}{18 \cdot S_{\mathrm{sub}}^{0.3}} \tag{5}$$

$$t_{\mathrm{ch}} = \frac{0.62 \cdot L \cdot n^{0.75}}{A^{0.125} \cdot S_{\mathrm{ch}}^{0.375}} \tag{6}$$

where L_{slp} is the average slope length for the sub-basin under consideration (m); n is the Manning coefficient for the sub-basin; S_{sub} is the average slope steepness of the sub-basin (m m^{-1}); L is the longest tributary length in the sub-basin (km); A denotes the area of the sub-basin (km^2); and S_{ch} is the average slope of the tributary channels within the sub-basin (m m^{-1}).

According to Eq. (2), the time base of the UH (t_{b}) is determined by both concentration time for the sub-basin (t_{c}) and shape adjustment factor (t_{adj}) concurrently. As seen in Fig. 1 and Table 2, there are obvious spatial differences of the geographical attributes among sub-basins. For instance, the values of sub-basin area vary from 2.94 km^2 to 4795.46 km^2 with the average value of 1437.12 km^2, and the mean slopes in source sub-basins (e.g. sub 1, sub 16, sub 19, sub 20 and sub 21) are much steeper than those in downstream sub-basins (e.g. sub 7, sub 8 and sub 11). As a result, the sub-basin concentration time t_c synthesizes all those geographical attributes and it can fully present the spatial differences among sub-basins according to Eq. (5) and (6). However, the parameter t_{adj} in Eq. (2) is a basin level parameter possessing a lumped value for all sub-basins, meaning that the spatial heterogeneity of t_b may be homogenized due to the constraints between sub-basins. Generally, the time base of triangular UH (t_b) should be reduced to produce increased peak flow for steep and small sub-basins, or increased to produce decreased peak flow for flat and large sub-basins. Thus, the shape adjustment parameter t_{adj} was modified from the basin level to the sub-basin level, and renamed t_{subadj} which allowed the UHs to be adjusted independently by distributed values.

3.3 Model calibration and validation

3.3.1 Sensitivity analysis

Sensitivity analysis is a process employed to identify the parameters that result in significant changes within a model output due to disturbances of the input (Holvoet et al., 2005). Generally, sensitivity analysis takes priority over the calibration process to reduce the complexity of the latter (Sudheer et al., 2011). Here, a combined Latin-Hypercube and One-factor-At-a-Time (LH-OAT) sampling method embedded within the SWAT model (Griensven et al., 2006) was used to conduct a sensitivity analysis. A total of 26 model parameters related to the flow simulation were involved in sensitivity analysis (see Appendix A). Only the most sensitive parameters were used for the optimization procedure, while the values of the others parameters were set to their default values.

3.3.2 Daily model calibration and validation

Due to the high spatial heterogeneity within the hydrological processes simulated by semi-distributed hydrological models, the values of numerous parameters will be difficult to determine by manual calibration alone. Therefore, the application of an automatic calibration process to estimate the model parameters that minimize the errors between the observed and simulated results is necessary. The Shuffled Complex Evolution (SCE-UA) algorithm (Duan et al., 1992) is a global optimization technique that is incorporated as a module into the SWAT model. In this study, the SWAT-EVENT model employed the same built-in automatic calibration subroutine. The SCE-UA algorithm has been applied to multiple physically based hydrological models (Sorooshian et al., 1993;Luce and Cundy, 1994;Gan and Biftu, 1996) and has exhibited good performance similar to other global search procedures (Cooper et al., 1997;Thyer et al., 1999;Kuczera, 1997;Jeon et al., 2014).

Daily simulations were performed within the time span, from 1990 to 2010, using observed data at the outlet of WJB. One year (1990) was selected as the model warm-up period, the period from 1991 to 2000 was used for the model calibration, and the remaining data from 2001 to 2010 were employed for validation.

Multiple statistical values, including the Nash-Sutcliffe efficiency coefficient (E_{NS}) (Nash and Sutcliffe, 1970), ratio of the root mean square error to the standard deviation of measured data (R_{SR}) (Singh et al., 2005) and the percent bias (P_{BIAS}) (Gupta et al., 1999), were selected in this study to evaluate the daily model performances, as shown in Eq. (7), (8) and (9). The E_{NS} provides a normalized statistic indicating how closely the observed and simulated data match with each other, wherein a value equal to 1 implies an optimal model performance insomuch that the simulated flow perfectly matches the observed flow. The R_{SR} index standardizes the root mean square error using the observations standard deviation, varying from 0 to a positive value. The optimal value of R_{SR} is 0, which indicates the perfect model simulation. The P_{BIAS} detects the degree that the simulated data deviates from the observed data.

$$E_{\mathrm{NS}} = 1 - \left[\frac{\sum_{i=1}^{n} \left(Q_{\mathrm{obs}}(i) - Q_{\mathrm{sim}}(i) \right)^2}{\sum_{i=1}^{n} \left(Q_{\mathrm{obs}}(i) - \overline{Q}_{\mathrm{obs}} \right)^2} \right] \tag{7}$$

$$R_{\mathrm{SR}} = \frac{\sqrt{\sum_{i=1}^{n} \left(Q_{\mathrm{obs}}(i) - Q_{\mathrm{sim}}(i) \right)^2}}{\sqrt{\sum_{i=1}^{n} \left(Q_{\mathrm{obs}}(i) - \overline{Q_{\mathrm{obs}}} \right)^2}} \tag{8}$$

$$P_{\mathrm{BIAS}} = \left[\frac{\sum_{i=1}^{n} \left(Q_{\mathrm{obs}}(i) - Q_{\mathrm{sim}}(i) \right) \cdot 100}{\sum_{i=1}^{n} Q_{\mathrm{obs}}(i)} \right] \tag{9}$$

where $Q_{\mathrm{obs}}(i)$ is the i th observed streamflow (m^3 s^{-1}); $Q_{\mathrm{sim}}(i)$ is the i th simulated streamflow (m^3 s^{-1}); n is the length of the time series.

3.3.3 Event-based sub-daily model calibration and validation

Sub-daily simulations in the SWAT-EVENT model were conducted within the same time span as the daily simulation, with a primary focus on the flood season with a series consisting of 24 flood events, two-thirds of which were utilized for the calibration while the rest were used for validation. Preferential implementation was applied to daily calibration from which the antecedent conditions were extracted.

Flow parameters, together with additional distributed parameters t_{subadj} associated with the UH method, were used for the sub-daily calibration. To analyze the influences of UH parameters on the SWAT-EVENT model performances, the lumped parameter t_{adj} was then calibrated while the other parameters remained unchanged exactly as the distributed case was calibrated. For the sub-basin level calibration, t_{subadj} was updated with distributed values for each of the sub-basins in each iteration; for the basin level calibration, t_{adj} was consistently updated with lumped values for all of the sub-basins in each iteration.

E_{NS}, relative peak discharge error (E_{RP}), relative peak time error (E_{RPT}) and relative runoff volume error (E_{RR}) were selected as the performance evaluation statistics for the flood event simulations to comply with the Accuracy Standard for Hydrological Forecasting in China (MWR, 2008). E_{RP} , E_{RPT} , and E_{RR} are specific indicators used to indicate whether the accuracies of the simulations reach the national standard (MWR, 2008). They are considered to be sufficiently qualified when the absolute values are less than 20 %, 20 % and 30 %, respectively.

4 Results

4.1 Daily simulation results

The model performances for daily streamflow simulations at outlet WJB are summarized in Table 3. The E_{NS} value is 0.80 for the calibration period and 0.83 for the validation period. These two values of the daily E_{NS} both exceed 0.75, which is considered to be good according to performance ratings for evaluation statistics recommended by Moriasi et al., (2007). The daily R_{SR} values are 0.45 and 0.42 for the calibration and validation, respectively, indicating that the root mean square error values are less than half the standard deviation of measured data, i.e. the "very good" model performances suggested by Moriasi et al. (2007). The SWAT model underestimates the streamflow by -14.32 % and -18.29 % for calibration and validation, respectively. Visual comparisons between the observed and simulated streamflows for both of the calibration and validation periods are shown in Fig. 5, from which it can be observed that the SWAT model could simulate well the temporal variation of streamflow at daily time scale. In general, the daily simulation results obtained from the SWAT model at WJB demonstrate decent applicability and can consequently represent a preliminary basis for further flood event simulation.

4.2 Event-based simulation results

The sub-daily simulation results for 24 flood events, as shown in Table 4, exhibit reliable performances of the SWAT-EVENT model, with E_{NS} values varying from 0.68 to 0.93, except for the event 19960917. The qualified ratios of E_{RP} , E_{RPT} and E_{RR} are 75%, 100% and 75%, respectively. Since the SWAT-EVENT model was developed on the base of the SWAT model, its superiority of the simulation in flood seasons was investigated by comparing those two model results for the same flood events. Table 4 also displays the model performances of the daily simulation results using the SWAT model for specific flood events. Most daily E_{NS} values are lower than the sub-daily ones, indicating that the flood hydrographs simulated by the sub-daily SWAT-EVENT model are much more reliable than those simulated by the daily SWAT model. In addition, the peak flows simulated by the SWAT-EVENT model on a sub-daily time scale are much closer to the observed flows relative to the predictions obtained from the SWAT model on a daily time scale, especially for flood events with high peak flows in Table 4. There are eight flood events (19910610, 19910629, 19960628, 20020622, 20030622, 20050707, 20050822 and 20070701) that exhibit peak flows greater than 5000 $m^3\ s^{-1}$. The sub-daily simulation results of these eight floods were aggregated into daily averages and then compared with those of the daily simulations, the results of which are illustrated in Fig. 6. It can be concluded that the daily simulations are likely to miss the high flood peaks. The more effective performances of the SWAT-EVENT model could be due to rainfall data with a higher temporal resolution and the model calculation with more detailed time steps, which can capture the instantaneous changes representative of flood processes.

All the statistical indicators suggest that the SWAT-EVENT model can accurately reproduce the dynamics of observed flood events based upon antecedent conditions extracted from SWAT daily simulations.

4.3 Effects of the UH parameters on the SWAT-EVENT model performances

To analyze the spatial variability of the UH parameters and their influences on the event-based flood simulation results, the time characteristics of the sub-basins as well as two sets of optimized UH parameters are displayed in Table 5. From Eq. (5) and Eq. (6), in addition to the geographic features of the sub-basins depicted in Table 2, the overland flow time t_{ov} and the channel flow time t_{ch} were calculated in Table 5. For the 21 sub-basins in studied catchment, the values of t_{ch} are always much greater than those of t_{ov}, implying that the channel flow time t_{ch} is the dominant factor that determines the total time of concentration t_{c} in Eq. (4). Due to the comprehensive function of longest tributary length, sub-basin area and average slope of the tributary channels in Table 2, the channel flow times (t_{ch}) are distributed in sub-basins, reaching the maximum (35.38 h) in sub-basin 16 and the minimum (1.12 h) in sub-basin 9.

The optimized sub-basin level UH parameters (t_{subadj}) are distributed in sub-basins, ranging from 0.48 h to 75.21 h, while the basin level parameters (t_{adj}) display a uniform value of 31.89 h for all sub-basins. As a consequence, the optimized t_{subadj} values enable the base time (t_{b}) and the peak time (t_{p}) of the UHs within the ranges of 6.38 h - 97.60 h and 2.39 h- 36.60 h, respectively. While for the basin level UH parameter case, the values of t_{b} and t_{p} distribute in a relatively narrow range, i.e. 33.54 h -54.28 h for t_{b} and 12.58 h - 20.35 h for t_{p}. The Coefficient of Variation (CV) in Table 5 was used to describe the spatial variability of the time characteristics of the UHs. As expected, the spatial variation of UHs derived by the sub-basin level parameters is 0.66, which is larger than the basin level case with the CV value of 0.13. Moreover, considering that the spatial CV of the concentration time t_{c} is 0.57, the spatial variation of the UHs calculated by the sub-basin UH parameters is deemed to be more reasonable. Though the UH time indicators (t_{b} and t_{p}) derived by the basin level UH parameter t_{adj} are always completely linear correlated to the concentration time t_{c} according to Eq. (2) and (3), its spatial variability could not be guaranteed. However, Fig. 7 still shows a correlation between t_{c} and t_{b} for the sub-basin level case, with higher t_{c}

generally having higher value of t_b. On this premise, the distributed UH parameters method makes the UH more accurate physical significance.

The SWAT-EVENT simulation results using the basin UH parameters are also presented in Table 4. Compared with the sub-basin level case, the sub-basin level case induces a decrease in the qualified ratio of E_{RP} from 75 % to 66.7 %, while keeping the same qualified ratio for E_{RPT} and E_{RR}. It can be conclude that changing the spatial level of the UH parameter affects the peak simulations significantly. In this procedure, model parameters except for the UH parameter remain fixed, thus there is little change in the specific values of E_{RR} between the two cases in Table 4. All these findings indicate that the application of sub-basin level UH parameters in the SWAT-EVENT model can improve the simulation accuracies of flood peaks.

The overall distributions of statistics for flood events for the two UH methods (i.e., the basin level UH parameter vs. the sub-basin level UH parameters) are plotted in Fig. 8. Since both cases fail to predict the event 19960917, of which the simulation result is excluded. The box plots therein exhibit rectangle heights equal to the interquartile range (IQR), the upper and lower ends of which are separately marked with the upper and lower quartile values, respectively. The median is represented by a line transecting either of the two rectangles. The extended whiskers denote the range of the batch data (Massart et al., 2005;Cox, 2009). According to Table 4 and Fig. 8, the SWAT-EVENT model simulated using sub-basin level UH parameters demonstrates improvements for event-based flood simulation. For the sub-basin level case in Fig. 8, half of the E_{NS} values range from 0.78 (lower quartile) to 0.90 (upper quartile), with a median of 0.87, which can potentially represent the second flood forecasting accuracy standard (i.e. B) according to MWR (MWR, 2008). However, the basin level case performs comparatively poorly with regard to reproducing the flood hydrograph, wherein the majority of E_{NS} values vary between 0.75 and 0.88. In comparison, the application of spatially distributed UH parameters allows the SWAT-EVENT model to simulate the flood events more accurately.

5 Discussion

Floods are always triggered by intense rainfall events with short duration. In order to adequately capture and analyze the rapid response of flood events, simulation time step is required at sub-daily resolution. Normally, an appropriate simulation time step is chosen depend on the observed catchment response time to a rainfall event. By examining the observed sub-daily rainfall and runoff time series at the WJB station, the general average response time between 1 day and 2 days. Moreover, considering the time interval of data acquisition (i.e. 2h to 6h), the 2-hour simulation step chosen in this study was more than sufficient for flood simulation. In an operational flood forecasting perspective, many endusers and practitioners are still in favor of the event-based models (Berthet et al., 2009). The emphasis on event-based modeling in this study was due to the unavailability of the long continuous hydrological data at sub-daily time scale. The data scarcity issue has also promoted the applications of the event-based models in some developing countries (Hughes, 2011;Tramblay et al., 2012). More broadly, the preferred event-based approach is highlighted when the hydrological model is used for more than flood prediction, for example the evaluation of the design floods and the estimation of urban storm water quantity and quality (Sansalone et al., 2005).

Several studies have declared that the catchment's antecedent moisture conditions prior to a flood event can have a strong influence on flood responses, including the flood volume, flood peak flow and its duration (Rodrã-Guez-Blanco et al., 2012;Tramblay et al., 2012;Coustau et al., 2012). Experimentally, the validation period was re-simulated by the SWAT-EVENT model when the antecedent moisture conditions were set to zero. The impact of antecedent soil moisture conditions on the event-based flood simulation results is presented in Fig. 9. The simulated flood hydrographs are comparatively lower when the antecedent conditions are initialized to zero relative to when they are extracted directly from the daily SWAT model. The flood volumes decrease accordingly. It is therefore rational to consider that accurate calculation of the antecedent moisture conditions is of crucial importance for the flood modeling. Since the major drawback of event-based models lies in its initialization: external information is needed to set the antecedent conditions of a catchment (Berthet et al., 2009;Tramblay et al., 2012). Numerous methods have been used to set up the initial conditions of event-based models, such as in-situ soil moisture measurements, retrieved soil moisture from the remote sensing products and continuous soil moisture modeling. Among these methods, continuous soil moisture modeling using the daily data series to estimate sub-daily initial conditions would be a traditional solution, as suggested by Nalbantis (1995). Tramblay et al. (2012) also tested different estimations of the antecedent moisture conditions of the catchment for an event-based hydrological model and concluded that the continuous daily soil moisture accounting method performed the best. However, there might be some deficiencies in the continuous simulation of the SWAT model in this study. On the one hand, the continuous SWAT model was calibrated using the sum of squares of the residuals as the objective function, which was more sensitive to high flows than low flows. As a consequence, the SWAT model ensured the simulation accuracy at the expense of the low flow performances, which would certainly bring errors to the estimations of antecedent moisture conditions. On the other hand, the continuous soil moisture modeling required long data series and took a long time to implement. Active microwave remote sensing has proved the feasibility and rationality of obtaining temporal and spatial soil moisture data. It means that there is a potential interest of using the remote sensing data to estimate the initial conditions (Tramblay et al., 2012).

Rainfall is the main driving force for the hydrological cycle. Hence, the temporal resolution of rainfall data could also have substantial impact on the simulation of flood processes. The decent performance of the SWAT-EVENT model at peak flows as shown in Fig. 6 could be due to the high temporal resolution of the input rainfall. Rainstorms may significantly vary over the course of a day, and thus, the use of daily rainfall data might not adequately represent the temporal profile. For example, a rainfall event (2 July 2003) prior to the peak of flood event 20030622 (Fig. 6) was characterized by an average daily rainfall of 80.6 mm for sub-basins located in the south part of study catchment, 85.24 % of which occurred during the first four time intervals ($\Delta t = 2$ h) between 0 and 8 am. The daily surface runoff was calculated using the SCS curve number method in the SWAT model, whereas the sub-daily surface runoff was calculated using the Green & Ampt infiltration method in the SWAT-EVENT model. On a daily basis, the Green & Ampt method will perform more effectively due to rainfall intensity and duration considerations. Similar results were analyzed through the comparison of the aforementioned two methods on the Goodwin Creek Watershed (Vol., 1999).

The UH represents the most widely practiced technique for determining flood hydrographs. Sherman (1932) first proposed the UH concept in 1932. However, because the UH proposed by Sherman is based on observed rainfall-runoff data at gauging sites for hydrograph derivations, it is only applicable for gauged basins (Jena and Tiwari, 2006). A prominent lack of observed data promoted the appearance of the Synthetic Unit Hydrograph (SUH), which extended the application of the UH technique to ungauged catchments. The triangular dimensionless UH used in this study denotes the simplest of SUHs, which relates hydrologic responses to the catchment geographic characteristics according to Eq. (2) - Eq. (6). There was a positive effect from the application of the distributed parameters of the UHs on the simulation of flood peaks as indicated in Table 4 and Fig. 8. However, due to the interaction between model parameters during the calibration procedure, not all sub-basin UH parameters would ensure the high linear relationship between the UH time base t_b and the sub-basin concentration time t_c in Fig. 7. From the calibrated results in Table 5, it was found that the optimized UH parameter in sub-basin 8 is unreasonably small. When sub-basin 8 was excluded, the coefficient of determination (r^2) in Fig. 7 would increase from 0.53 to 0.69. Optimization, admittedly, is not the only solution to obtain the UH parameters. Jena and Tiwari (2006) developed regression equations between individual UH parameters and geomorphologic parameters of the watershed. In addition to the triangular dimensionless UH used in this study, there are many other available methods for derivation of the SUH. Bhunya et al. (2007) compared four probability distribution functions (pdfs) in developing SUH and concluded that such statistical distributions method performed better than the traditional synthetic methods. There might be room for further improving the current UH method used in the SWAT-EVENT model.

6 Conclusions

Flood forecasting is a synthetic system that integrates the data acquisition and processing, rainfall-runoff modeling and warning information release etc. Hydrological models are always the core part of the forecasting system. Model structures and parameters are one of the most important issues for accurate flood forecasting (Noh et al., 2014). The original SWAT model was not competent to flood forecasting due to its initial design of long-term simulations with daily time-steps. This paper mainly focused on the modification of the structure of the original SWAT model to perform event-based simulation, which was applicable for the area without continuous long-term observations. The newly developed SWA-EVENT model was applied in the upper reaches of the Huaihe River. Model calibration and validation were made by the using of historical flood events, showing good simulation accuracy. To improve the spatial representation of the SWA-EVENT, the lumped UH parameters were then adjusted to the distributed ones. Calibration and validation results revealed the improvement of event-based simulation performances. This study expands the application of the original SWAT model in event-based flood simulation.

The determination of hydrological model parameters is an inevitable process before flood forecasting. Parameter estimations of distributed or semi-distributed hydrological models commonly depend on automated calibration procedure due to overparametrization. The optimal parameters of the SWAT-EVENT model were obtained by the automatic parameter calibration module that integrated SCE-UA algorithm in this study. However, serveral factors such as interactions among model parameters, complexities of spatio-temporal scales and statistical features of model residuals may lead to the parameter non-uniqueness, which is the source of the uncertainty in the estimated parameters. Uncertainty of model parameters will be finally passed to the model results, hence leading to certain risks in flood forecasting. In the future, emphasis will be placed on the quantification of the parameter uncertainty to provide better supports for flood operations.

Event-based runoff quantity and quality modeling has become a challenge task since the impact of hydrological extremes on the water quality is particularly important. The improvement of the SWAT model for event-based flood simulation will lay the foundation for dealing with the event-based water quality issues.

Data availability

The DEM data were downloaded from the website http://srtm.csi.cgiar.org/.

The land use data (GLC2000) were downloaded from the website http://www.landcover.org/.

The soil data (HWSD) were downloaded from the website http://webarchive.iiasa.ac.at/Research/LUC/External-World-soil-database/HTML/.

The global weather data were downloaded from the website https://globalweather.tamu.edu/.

The rainfall observations at 138 stations and the discharge observations at the outlet (WJB) were provided by Hydrologic Bureau of Huaihe River Commission.

The source codes of SWAT model are available at the website http://swat.tamu.edu/.

Appendix A

Table A 1 Flow simulation related parameters and their lower bound and upper bound in the SWAT model, and the additional UH parameters for the SWAT-EVENT model.

Parameters	Definition	lower bound	upper bound
ALPHA_BF	Baseflow alpha factor (days).	0	1
BIOMIX	Biological mixing efficiency.	0	1
BLAI	Maximum potential leaf area index.	0	1
CANMX	Maximum canopy storage (mm H2O).	0	10
CH_K(2)	Effective hydraulic conductivity in main channel alluvium (mm/hr).	0	150
CH_N	Manning's "n" value for the main channel.	0	1
CN2	Initial SCS runoff curve number for moisture condition II.	-50	50
EPCO	Plant uptake compensation factor.	0	1
ESCO	Soil evaporation compensation factor	0	1
GW_DELAY	Groundwater delay time (days).	-10	10
GW_REVAP	Groundwater "revap" coefficient.	-0.036	0.036
GWQMN	Threshold depth of water inthe shallow aquifer required for return flow to occur (mm H2O).	-1000	1000
REVAPMN	Threshold depth of water in the shallow aquifer for “revap” or percolation to the deep aquifer to occur (mm H2O).	-100	100
SMTMP	Snow melt base temperature (ºC).	0	5
SLOPE	Average slope	-25	25
SLSUBBSN	Average slope length (m).	-25	25
SMFMN	Melt factor for snow on December 21 (mm H2O/ºC-day).	0	10
SMFMX	Melt factor for snow on June 21 (mm H2O/ºC-day).	0	10
SMTMP	Snow melt base temperature (ºC).	-25	25
SOL_ALB	Moist soil albedo.	-25	25
SOL_AWC	Available water capacity of the soil layer (mm H2O/mm soil).	-50	50
SOL_K	Saturated hydraulic conductivity (mm/hr).	-25	25
SOL_Z	Depth from soil surface to bottom of layer (mm).	-40	40
SURLAG	Surface runoff lag coefficient.	0	10
TIMP	Snow pack temperature lag factor.	0	1
TLAPS	Temperature lapse rate (ºC/km).	0	50
t_{adj}	Basin level UH parameter (h)	0	100
t_{subadj}	Sub-basin level UH parameter (h)	0	130

Table A 2 The optimal parameters for the SWAT model and the SWAT-EVENT model.

Prameters	Daily simulation with SWAT model	Event-based simulation with SWAT-EVENT model
Alpha_Bf	0.84	0.96
Blai	1.00	0.31
Ch_K2	70.99	0.37
Ch_N	0.16	0.02
Cn2	9.00	47.75
Esco	0.96	0.22
Revapmin	-83.91	-92.27
Sol_Awc	49.47	-1.13
Sol_Z	12.94	35.14
Surlag	2.25	0.22
t_{adj}		0.48~75.21
t_{subadj}		31.89

Competing interests

The authors declare that they have no conflict of interest.

Acknowledgments

This research has been supported by Non-profit Industry Financial Program of Ministry of Water Resources of China (No. 201301066), National key research and development program (2016YFC0402700), the National Natural Science Foundation of China (No. 91547205, 51579181, 51409152, 41101511, 40701024), and Hubei Provincial Collaborative Innovation Center for Water Security.

References

Adams Iii, T. E., and Pagano, T. C.: Flood Forecasting: A Global Perspective, in: Flood Forecasting, Academic Press, Boston, xxiii-xlix, 2016.

Aron, G., and White, E. L.: Fitting a Gamma Distribution Over a Synthetic Unit Hydrograph, JAWRA Journal of the American Water Resources Association, 18, 95-98, 1982.

Bartholomé, E., and Belward, A. S.: GLC2000: a new approach to global land cover mapping from Earth observation data, International Journal of Remote Sensing, 26, 1959-1977, 2005.

Berthet, L., Andréassian, V., Perrin, C., and Javelle, P.: How crucial is it to account for the antecedent moisture conditions in flood forecasting? Comparison of event-based and continuous approaches on 178 catchments, Hydrology & Earth System Sciences, 13, 819-831, 2009.

BEVEN, K. J., and KIRKBY, M. J.: A physically based, variable contributing area model of basin hydrology / Un modèle à base physique de zone d'appel variable de l'hydrologie du bassin versant, Hydrological Sciences Bulletin, 24, 43-69, 1979.

Bhunya, P. K., Berndtsson, R., Ojha, C. S. P., and Mishra, S. K.: Suitability of Gamma, Chi-square, Weibull, and Beta distributions as synthetic unit hydrographs, J. Hydrol., 334, 28-38, 2007.

Bhunya, P. K.: Synthetic Unit Hydrograph Methods: A Critical Review, Open Hydrology Journal, 5, 1-8, 2011.

Cooper, V. A., Nguyen, V. T. V., and Nicell, J. A.: Evaluation of global optimization methods for conceptual rainfall-runoff model calibration, Water Science & Technology, 36, 53-60, 1997.

Coustau, M., Bouvier, C., Borrellestupina, V., and Jourde, H.: Flood modelling with a distributed event-based parsimonious rainfall-runoff model: case of the karstic Lez river catchment, Natural Hazards & Earth System Sciences, 12, 1119-1133, 2012.

Cox, N. J.: Speaking Stata: Creating and varying box plots, Stata Journal, 9, 478-496, 2009.

Duan, Q., Soroosh, S., and Vijai, G.: Effective and efficient global optimization for conceptual rainfall-runoff models, Water Resources Research, 28, 1015-1031, 1992.

Gan, T. Y., and Biftu, G. F.: Automatic Calibration of Conceptual Rainfall-Runoff Models: Optimization Algorithms, Catchment Conditions, and Model Structure, Water Resources Research, 32, 3513-3524, 1996.

Gassman, P. W., Arnold, J. J., Srinivasan, R., and Reyes, M.: The Worldwide Use of the SWAT Model: Technological Drivers, Networking Impacts, and Simulation Trends, Century Watershed Technology: Improving Water Quality and Environment Conference Proceedings, 21-24 February 2010, Universidad Earth, Costa Rica, 2010,

Griensven, A. V., Meixner, T., Grunwald, S., Bishop, T., Diluzio, M., and Srinivasan, R.: A global sensitivity analysis tool for the parameters of multi-variable catchment models, J. Hydrol., 324, 10-23, 2006.

Gupta, H. V., Sorooshian, S., and Yapo, P. O.: Status of Automatic Calibration for Hydrologic Models: Comparison With Multilevel Expert Calibration, Journal of hydrologic Engineering, 4, 135-143, 1999.

Hapuarachchi, H. A. P., Wang, Q. J., and Pagano, T. C.: A review of advances in flash flood forecasting, Hydrol. Process., 25, 2771-2784, 2011.

Holvoet, K., Griensven, A. V., Seuntjens, P., and Vanrolleghem, P. A.: Sensitivity analysis for hydrology and pesticide supply towards the river in SWAT, Physics & Chemistry of the Earth Parts A/b/c, 30, 518-526, 2005.

Hughes, D. A.: Regionalization of models for operational purposes in developing countries: an introduction, Hydrology Research, 42, 331, 2011.

Jena, S. K., and Tiwari, K. N.: Modeling synthetic unit hydrograph parameters with geomorphologic parameters of watersheds, J. Hydrol., 319, 1-14, 2006.

Jeon, J. H., Park, C. G., and Engel, B. A.: Comparison of Performance between Genetic Algorithm and SCE-UA for Calibration of SCS-CN Surface Runoff Simulation, Water, 6, 3433-3456, 2014.

Jeong, J., Kannan, N., Arnold, J., Glick, R., Gosselink, L., and Srinivasan, R.: Development and Integration of Sub-hourly RainfallRunoff Modeling Capability Within a Watershed Model, General Information, 24, 4505-4527, 2010.

Jeong, J., Kannan, N., Arnold, J. G., Glick, R., Gosselink, L., Srinivasan, R., and Harmel, R. D.: DEVELOPMENT OF SUB - DAILY EROSION AND SEDIMENT TRANSPORT ALGORITHMS FOR SWAT, Transactions of the Asabe, 54, 1685-1691, 2011.

Jiang, X. F., Wang, L., Fang, M. A., Hai-Qiang, L. I., Zhang, S. J., and Liang, X. W.: Localization Method for SWAT Model Soil Database Based on HWSD, China Water & Wastewater, 30, 135-138, 2014.

Kiniry, J. R., Williams, J. R., and King, K. W.: Soil and Water Assessment Tool Theoretical Documentation (Version 2005), Computer Speech & Language, 24, 289-306, 2005.

Kuczera, G.: Efficient subspace probabilistic parameter optimization for catchment models, Water Resources Research, 33, 177–185, 1997.

Luce, C. H., and Cundy, T. W.: Parameter Identification for a Runoff Model for Forest Roads, Water Resources Research, 30, 1057-1070, 1994.

Maidment, D. R.: handbook of hydrology, Earth-Science Reviews, 24, 227–229, 1994.

Massart, D. L., Smeyers-Verbeke, J., Capron, X., and Schlesier, K.: Visual presentation of data by means of box plots, Lc Gc Europe, 18, 215-218, 2005.

Mendes, J., and Maia, R.: Hydrologic Modelling Calibration for Operational Flood Forecasting, Water Resour. Manag., 30, 1-15, 2017.

Moriasi, D. N., Arnold, J. G., Van Liew, M. W., Bingner, R. L., Harmel, R. D., and Veith, T. L.: Model evaluation guidelines for systematic quantification of accuracy in watershed simulations, Transactions of the Asabe, 50, 885-900, 2007.

Nachtergaele, F. O., Velthuizen, Verelst, L., Batjes, N. H., Dijkshoorn, J. A., Engelen, V., W. P., Fischer, G., Jones, A., and Montanarella, L.: Harmonized World Soil Database (Version 1.2), Laxenburg, Austria : Food and Agriculture Organization of the UN, International Institute for Applied Systems Analysis, ISRIC - World Soil Information, Institute of Soil Science - Chinese Academy of Sciences, Joint Research Centre of the EC, 2012 - p, 2012.

Nalbantis, I.: Use of multiple-time-step information in rainfall-runoff modelling, J. Hydrol., 165, 135-159, http://dx.doi.org/10.1016/0022-1694(94)02567-U, 1995.

Nash, J. E., and Sutcliffe, J. V.: River flow forecasting through conceptual models part I — A discussion of principles J. Hydrol., 10, 282-290, 1970.

Neitsch, S. L., Arnold, J. G., Kiniry, J. R., Srinivasan, R., and Williams, J. R.: Soil and Water Assessment Tool Input/output File Documentation: Version 2009. Texas Water Resources Institute Technical Report 365, Journal of Information Processing and Management, 33, 2011.

Noh, S. J., Rakovec, O., Weerts, A. H., and Tachikawa, Y.: On noise specification in data assimilation schemes for improved flood forecasting using distributed hydrological models, J. Hydrol., 519, 2707-2721, 2014.

Rodrã-Guez-Blanco, M. L., Taboada-Castro, M. M., and Taboada-Castro, M. T.: Rainfallâ "runoff response and event-based runoff coefficients in a humid area (northwest Spain), International Association of Scientific Hydrology Bulletin, 57, 445-459, 2012.

Romanowicz, A. A., Vanclooster, M., Rounsevell, M., and Junesse, I. L.: Sensitivity of the SWAT model to the soil and land use data parametrisation: a case study in the Thyle catchment, Belgium, Ecological Modelling, 187, 27-39, 2005.

Sansalone, J. J., Hird, J. P., Cartledge, F. K., and Tittlebaum, M. E.: Event-based stormwater quality and quantity loadings from elevated urban infrastructure affected by transportation, Water Environment Research, 77, 348-365, 2005.

SCS: National engineering handbook, section 4, hydrology., in, US Department of Agriculture,SCS, Washington, DC, 1972.

Sherman, L.: Stream Flow from Rainfall by the Unit-Graph Method, 1932.

Singh, J., Knapp, H. V., Arnold, J. G., and Demissie, M.: HYDROLOGICAL MODELING OF THE IROQUOIS RIVER WATERSHED USING HSPF AND SWAT, JAWRA Journal of the American Water Resources Association, 41, 343-360, 2005.

Singh, V. P.: Computer models of watershed hydrology, Computer Models of Watershed Hydrology, 443-476, 1997.

Sorooshian, S., Duan, Q., and Gupta, V. K.: Calibration of rainfall-runoff models: Application of global optimization to the Sacramento Soil Moisture Accounting Model, Water Resources Research, 29, 1185-1194, 1993.

Sudheer, K. P., Lakshmi, G., and Chaubey, I.: Application of a pseudo simulator to evaluate the sensitivity of parameters in complex watershed models, Environ. Modell. Softw., 26, 135-143, http://dx.doi.org/10.1016/j.envsoft.2010.07.007, 2011.

Thyer, M., Kuczera, G., and Bates, B. C.: Probabilistic optimization for conceptual rainfall-runoff models: A comparison of the shuffled complex evolution and simulated annealing algorithms, Water Resources Research, 35, 767–773, 1999.

Tramblay, Y., Bouaicha, R., Brocca, L., Dorigo, W., Bouvier, C., Camici, S., and Servat, E.: Estimation of antecedent wetness conditions for flood modelling in northern Morocco, Hydrology & Earth System Sciences Discussions, 9, 4375-4386, 2012.

Vol., N.: COMPARISON OF GREEN-AMPT AND CURVE NUMBER METHODS ON GOODWIN CREEK WATERSHED USING SWAT, Transactions of the ASAE, 42, 919-926, 1999.

Xiong, L., and Guo, S.: Effects of the catchment runoff coefficient on the performance of TOPMODEL in rainfall–runoff modelling, Hydrol. Process., 18, 1823–1836, 2004.

Yao, C., Zhang, K., Yu, Z., Li, Z., and Li, Q.: Improving the flood prediction capability of the Xinanjiang model in ungauged nested catchments by coupling it with the geomorphologic instantaneous unit hydrograph, J. Hydrol., 517, 1035-1048, http://dx.doi.org/10.1016/j.jhydrol.2014.06.037, 2014.

Yao, H., Hashino, M., Terakawa, A., and Suzuki, T.: COMPARISON OF DISTRIBUTED AND LUMPED HYDROLOGICAL MODELS, Doboku Gakkai Ronbunshuu B, 42, 163-168, 1998.

Zhao, L. N., Tian, F. Y., Wu, H., Qi, D., Di, J. Y., and Wang, Z.: Verification and comparison of probabilistic precipitation forecasts using the TIGGE data in the upriver of Huaihe Basin, Advances in Geosciences, 29, 95-102, 2011.

Table 1 SWAT model input data and sources for the Wangjiaba (WJB) catchment.

Data type	Resolution	Source	Description
DEM	90m×90m	http://srtm.csi.cgiar.org/	Digital Elevation Model
Land use	1km×1km	http://www.landcover.org/	Land use classification
Soil	30 arc-second	http://www.fao.org/soils-portal/soil-survey/soil-maps-and-databases/harmonized-world-soil-database-v12/en/	Soil type classification and characterization of soil parameters
Global weather data	30 stations	https://globalweather.tamu.edu/	Relative humidity, wind speed, solar radiation and the minimum and maximum air temperatures
Observed rainfall	138 gauges	Hydrologic Bureau of Huaihe River Commission	Daily data: 1991-2010; sub-daily data: flood periods during 1991-2010
Observed streamflow	1 gauges	Hydrologic Bureau of Huaihe River Commission	Wangjiaba station, daily data for 1991-2010, sub-daily data for flood periods during 1991-2010

Table 2 Geographic features of sub-basins for the Wangjiaba (WJB) catchment.

Sub-basin No.	Drainage area (km^2)	Mean elevation (m)	Mean slope (°)	Mean slope length (m)	Longest tributary length (km)	Average slope of the tributary ($m\ m^{-1}$)
1	1997.74	83	7.49	60.96	140.06	0.0010
2	262.15	62	1.05	121.91	49.46	0.0001
3	1032.38	60	1.41	121.91	130.46	0.0010
4	2515.71	161	4.58	91.44	175.31	0.0040
5	1712.57	42	1.20	121.91	121.25	0.0010
6	3852.86	57	2.71	91.44	295.11	0.0010
7	4.26	30	1.32	121.91	4.13	0.0010
8	722.28	32	0.93	121.91	81.10	0.0001
9	2.94	32	2.26	91.44	4.92	0.0020
10	927.36	49	0.95	121.91	101.10	0.0010
11	450.41	31	1.12	121.91	73.08	0.0001
12	31.34	35	1.59	121.91	16.31	0.0010
13	477.56	47	0.88	121.91	48.86	0.0001
14	295.68	49	1.13	121.91	42.90	0.0010
15	886.69	54	1.10	121.91	104.65	0.0010
16	4795.46	96	7.28	60.96	209.67	0.0020
17	999.62	57	3.68	91.44	95.88	0.0040
18	2216.48	50	4.43	91.44	141.88	0.0030
19	2029.25	148	13.17	24.38	170.84	0.0040
20	2399.24	74	8.42	60.96	160.71	0.0060
21	2567.61	100	8.80	60.96	120.53	0.0060

Table 3 SWAT model performance statistics for the calibration and validation periods.

	E_{NS}	R_{SR}	P_{BIAS} (%)
Calibration	0.80	0.45	-14.32
Validation	0.83	0.42	-18.29

Table 4 Performance evaluations for the daily simulation with the SWAT model for specific flood events, and the SWAT-EVENT model performances with sub-basin level UH parameters and basin level UH parameter.

	Flood event	Start date	End date	Observed peak flow	Daily simulation with SWAT model		SWAT-EVENT model with sub-basin level UH parameters					SWAT-EVENT model with basin level UH parameter				
					Simulated peak flow	E_{NS}	Simulated peak flow	E_{RP}	E_{RPT}	E_{RR}	E_{NS}	Simulated peak flow	E_{RP}	E_{RPT}	E_{RR}	E_{NS}
				($m^3 s^{-1}$)	($m^3 s^{-1}$)		($m^3 s^{-1}$)	(%)	(%)	(%)		($m^3 s^{-1}$)	(%)	(%)	(%)	
Calibration	19910521	21-May	10-Jun	2935	1720	0.58	2350	-19.93	-6.04	-9.84	0.87	2520	-14.14	-7.38	-9.99	0.87
	19910610	10-Jun	29-Jun	7577	4690	0.80	6210	-18.04	0.00	-14.82	0.93	6360	-16.06	2.70	-14.75	0.94
	19910629	29-Jun	21-Jul	5931	3870	0.85	4880	-17.72	-2.63	-15.46	0.90	4740	-20.08	1.75	-15.46	0.86
	19910804	4-Aug	17-Aug	4824	3340	0.74	4030	-16.46	-4.76	-5.03	0.89	4350	-9.83	-6.35	-4.61	0.89
	19950707	7-Jul	18-Jul	2613	2250	0.59	3560	36.24	-7.32	38.15	0.87	3250	24.38	-14.63	38.15	0.85
	19950803	3-Aug	6-Sep	922.1	995	0.69	1280	38.81	-8.02	39.00	0.72	1270	37.73	-4.40	39.02	0.71
	19960628	28-Jun	25-Jul	5298	3280	0.30	4810	-9.21	-1.53	-1.42	0.68	4870	-8.08	-1.15	-1.33	0.66
	19960917	17-Sep	26-Sep	1239	1490	0.79	1560	25.91	9.76	17.06	0.19	1640	32.36	9.76	18.32	0.17
	19970629	29-Jun	30-Jul	2171	1340	0.82	2360	8.71	12.05	35.79	0.73	2550	17.46	8.93	36.22	0.63
	19980630	30-Jun	13-Jul	4504	3070	0.77	4350	-3.42	-4.92	-13.56	0.78	4370	-2.98	-3.28	-13.49	0.74
	19980725	25-Jul	2-Sep	3698	3360	0.81	3180	-14.01	-5.96	-15.78	0.91	3750	1.41	-7.28	-15.66	0.93
	20020622	22-Jun	11-Jul	5715	4170	0.75	7050	23.36	-8.16	35.38	0.87	7960	39.28	-10.20	35.49	0.82
	20020722	22-Jul	4-Aug	4088	3290	0.73	3850	-10.26	-10.20	-20.61	0.89	4220	-1.63	-10.20	-20.39	0.89
	20030622	22-Jun	29-Jul	8740	4940	0.68	5690	-34.90	-3.73	-9.98	0.84	6150	-29.63	-3.73	-10.25	0.80
	20040717	17-Jul	29-Jul	2229	2080	0.27	1920	-13.86	-6.12	14.92	0.82	2100	-5.79	-10.20	15.47	0.85
	20040804	4-Aug	13-Aug	2641	2280	0.67	2890	9.43	-16.33	7.81	0.80	2720	2.99	-16.33	8.99	0.78
Validation	20050707	7-Jul	12-Aug	7331	4320	0.65	6290	-14.20	-11.84	-16.11	0.83	6530	-10.93	-9.21	-16.13	0.86
	20050822	22-Aug	10-Sep	5650	3330	0.45	3990	-29.38	0.00	-33.02	0.69	4260	-24.60	-0.83	-32.94	0.73
	20060722	22-Jul	16-Aug	1770	1270	0.83	1450	-18.08	10.00	-14.08	0.81	1670	-5.65	5.45	-13.90	0.84

	20070701	1-Jul	1-Aug	7926	5780	0.74	6550	-17.36	-7.32	-19.51	0.91	6820	-13.95	-6.50	-19.32	0.91
	20080722	22-Jul	9-Aug	4264	3120	0.68	4250	-0.33	6.12	8.67	0.92	4370	2.49	2.04	8.72	0.90
	20080814	14-Aug	27-Aug	4219	2730	0.69	3380	-19.89	-4.84	-8.19	0.88	3590	-14.91	-4.84	-7.75	0.88
	20090826	26-Aug	13-Sep	2221	2030	0.72	2590	16.61	1.39	35.41	0.72	2790	25.62	-1.39	35.63	0.75
	20100712	12-Jul	5-Aug	4314	2930	0.87	4290	-0.56	-1.75	-9.79	0.92	4300	-0.32	-0.88	-9.72	0.93
Qualified (%)								75	100	75			66.67	100.00	75.00	

Table 5 Time characteristics of the sub-basins (tc, tb, tp) and the optimized UH parameters for each sub-basin.

Sub-basin	t_{ov} (h)	t_{ch} (h)	t_c (h)	Sub-basin level UH parameters			Basin level UH parameters		
				t_{subadj} (h)	t_b (h)	t_p (h)	t_{adj} (h)	t_b (h)	t_p (h)
1	1.12	18.23	19.35	16.69	28.80	10.80		44.00	16.50
2	0.40	19.68	20.08	51.24	63.78	23.92		44.44	16.66
3	1.15	18.44	19.59	45.77	58.02	21.76		44.14	16.55
4	1.12	13.18	14.30	1.90	10.98	4.12		40.97	15.36
5	1.12	16.09	17.21	37.67	48.50	18.19		42.72	16.02
6	1.10	35.38	36.48	75.21	97.60	36.60		54.28	20.35
7	1.15	1.16	2.31	6.07	7.96	2.98		33.78	12.67
8	1.25	28.42	29.68	9.40	27.70	10.39		50.20	18.82
9	0.80	1.12	1.91	4.73	6.38	2.39		33.54	12.58
10	1.21	14.48	15.70	51.17	61.09	22.91		41.81	15.68
11	1.25	27.17	28.42	62.16	79.71	29.89	31.89	49.44	18.54
12	1.04	3.57	4.60	8.53	11.79	4.42		35.15	13.18
13	1.30	18.03	19.33	53.32	65.42	24.53		43.99	16.50
14	1.25	7.09	8.34	27.62	33.12	12.42		37.40	14.02
15	1.21	15.07	16.29	0.48	10.75	4.03		42.16	15.81
16	0.74	18.86	19.60	63.50	75.76	28.41		44.15	16.56
17	0.76	8.09	8.85	25.75	31.55	11.83		37.70	14.14
18	0.81	12.07	12.88	39.83	48.06	18.02		40.12	15.04
19	0.69	13.19	13.88	45.37	54.20	20.33		40.72	15.27
20	0.14	10.44	10.58	6.19	13.04	4.89		38.74	14.53
21	0.16	7.76	7.92	20.43	25.68	9.63		37.14	13.93
CV	0.38	0.60	0.57		0.66	0.66		0.13	0.13

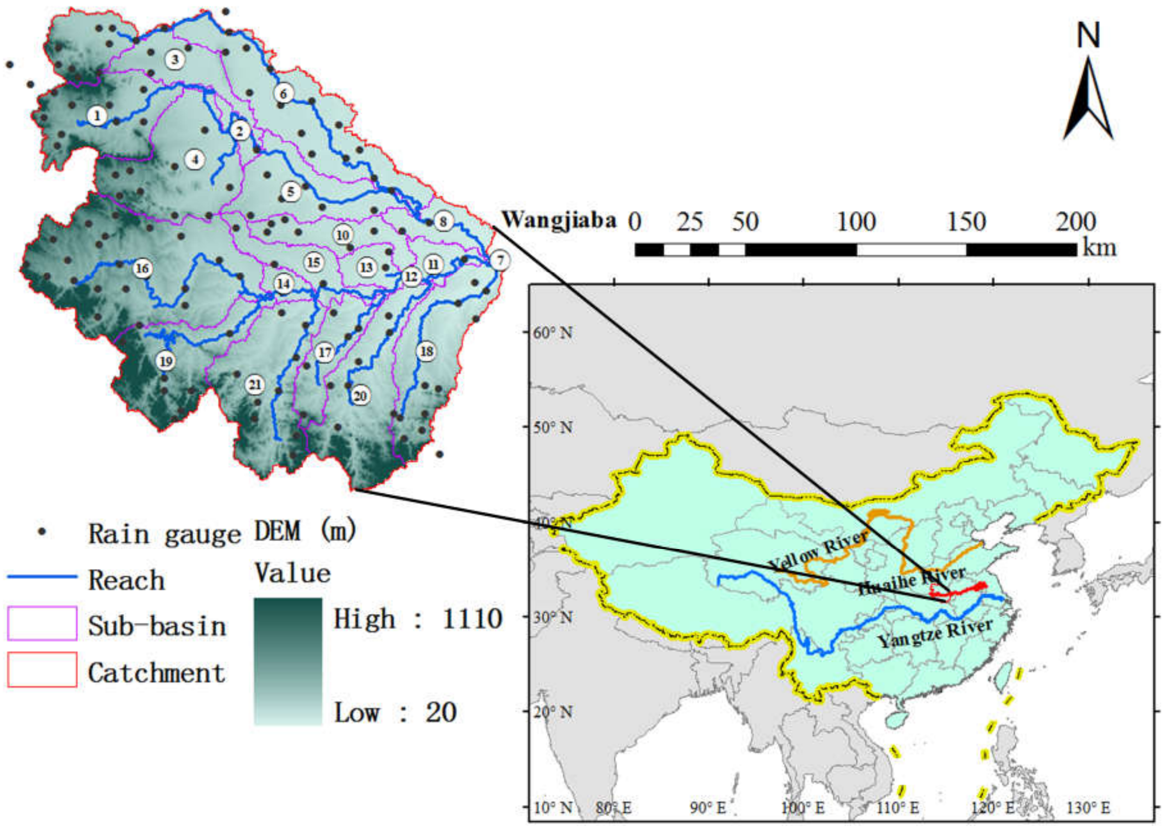

Figure 1 The Wangjiaba (WJB) catchment.

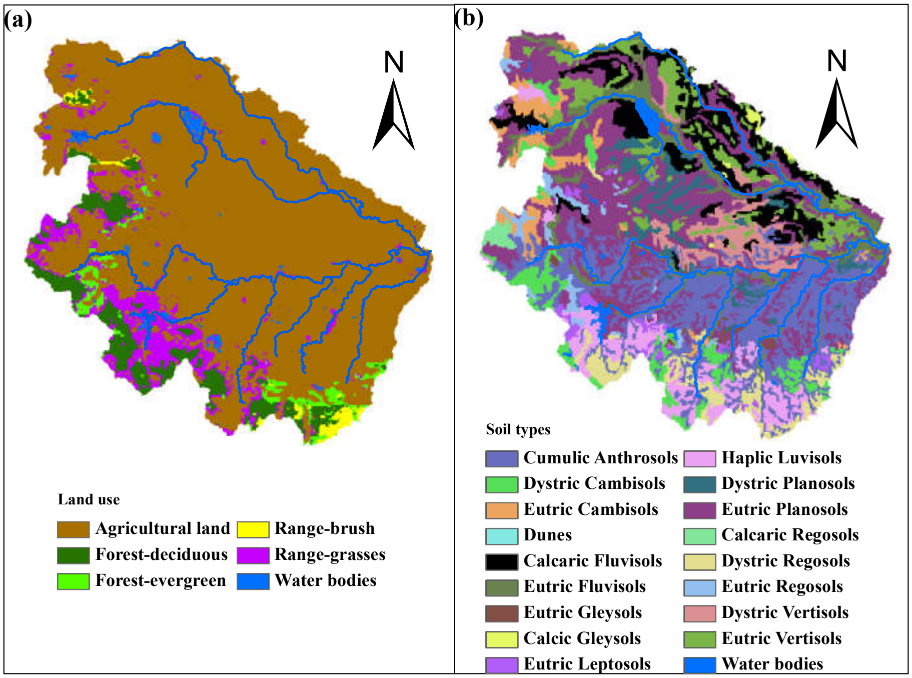

Figure 2 (a) Land use and (b) soil types throughout the study area.

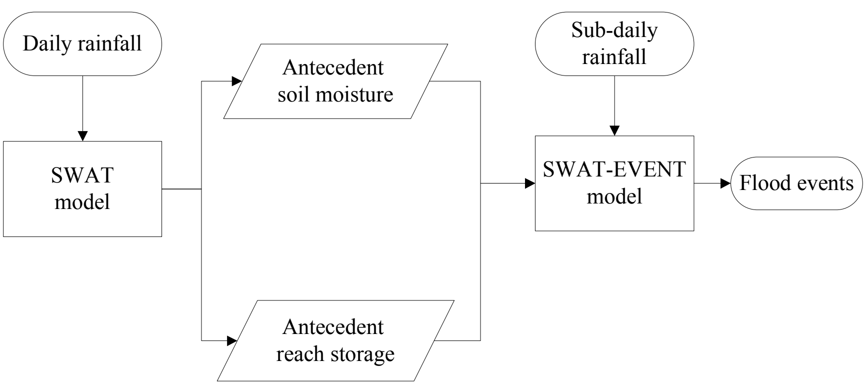

Figure 3 SWAT-EVENT model for the simulation of event-based flood data based on the initial conditions extracted from daily simulation results produced by the original SWAT model.

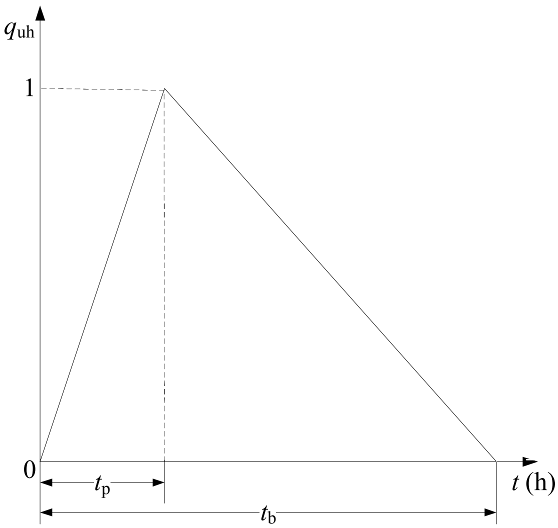

Figure 4 Shape of the dimensionless triangular UH.

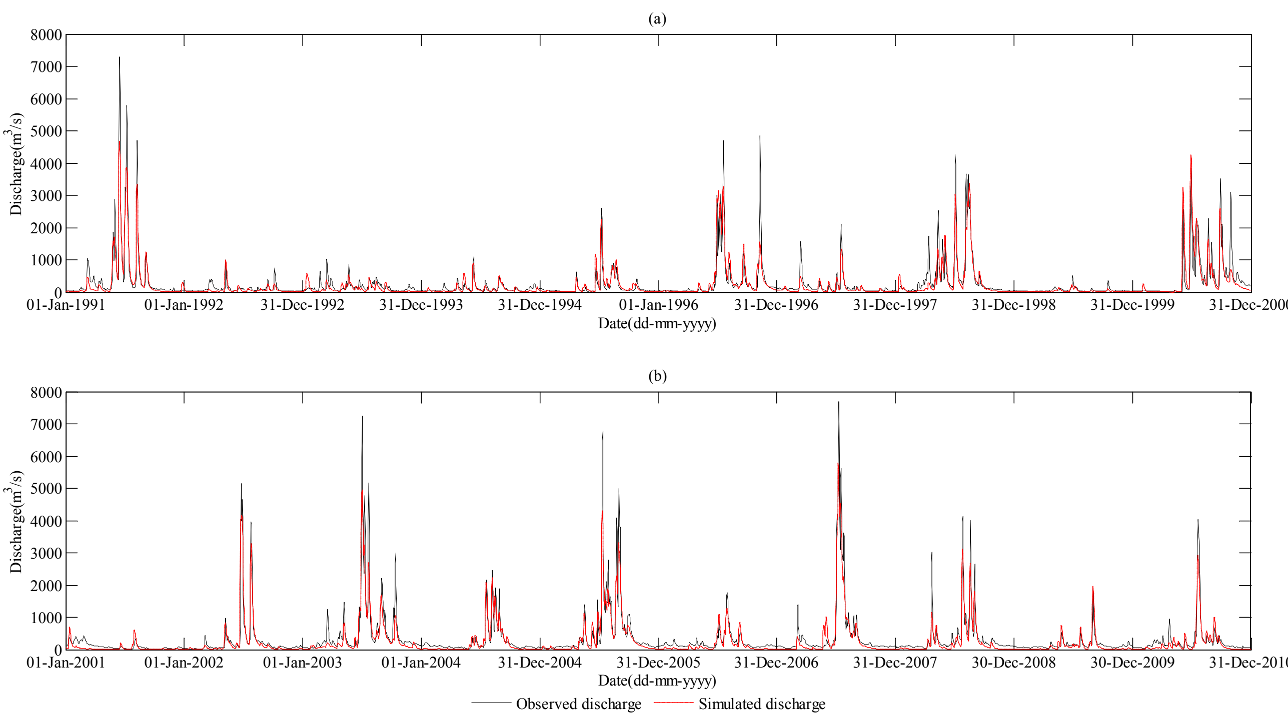

Figure 5 Comparisons between the observed and simulated daily discharges for the calibration and validation periods at WJB.

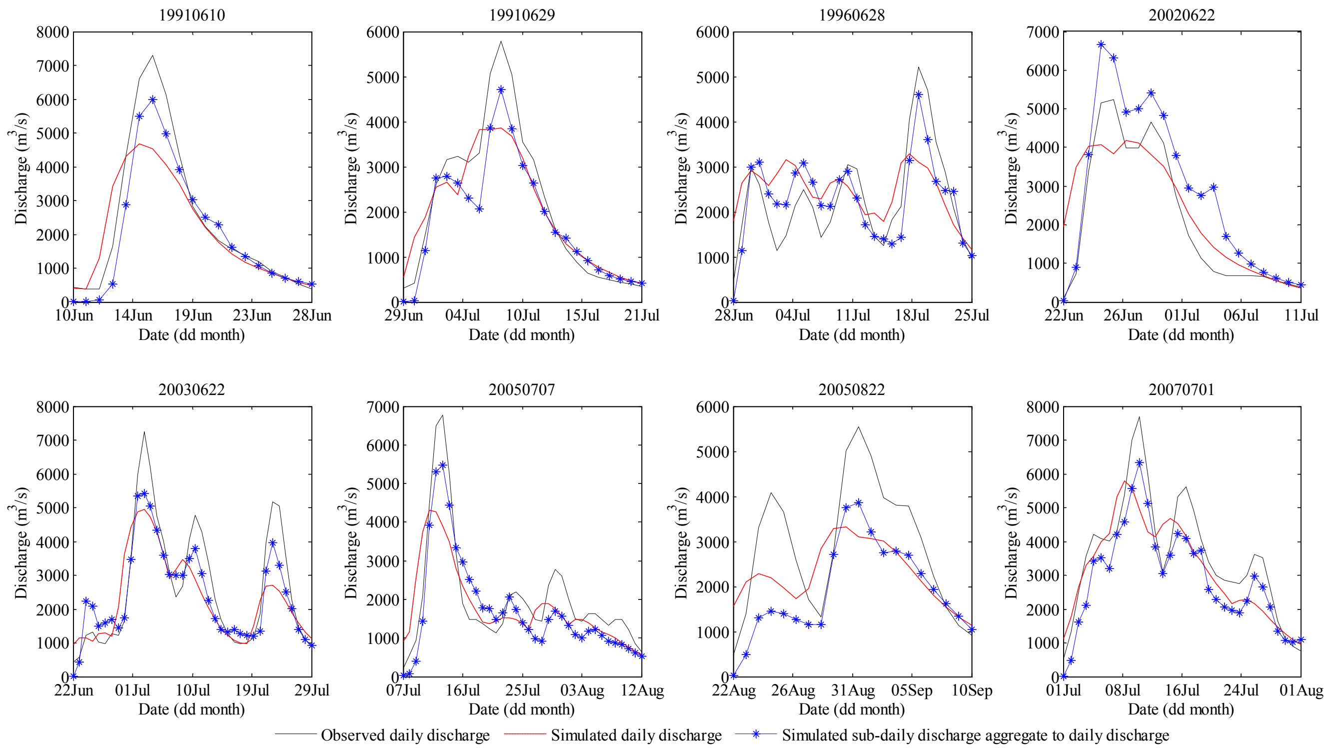

Figure 6 Comparisons of the daily simulations conducted using the SWAT model and the aggregated sub-daily simulations conducted using the SWAT-EVENT model.

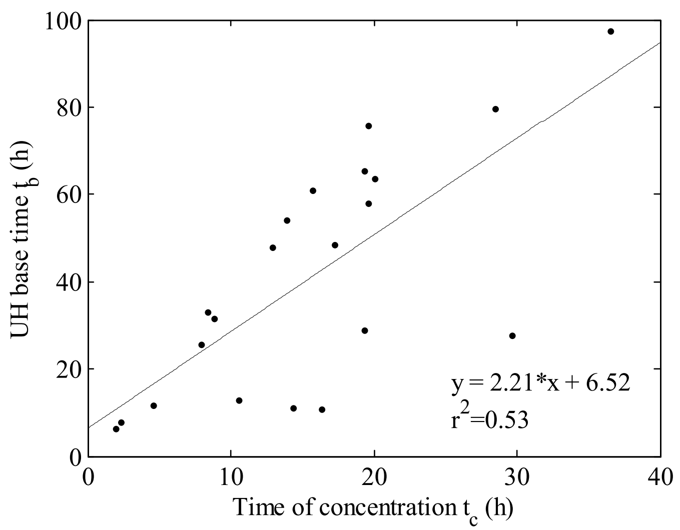

Figure 7 Relationship between UH time base t_b and concentration time t_c, with a coefficient of determination (r^2).

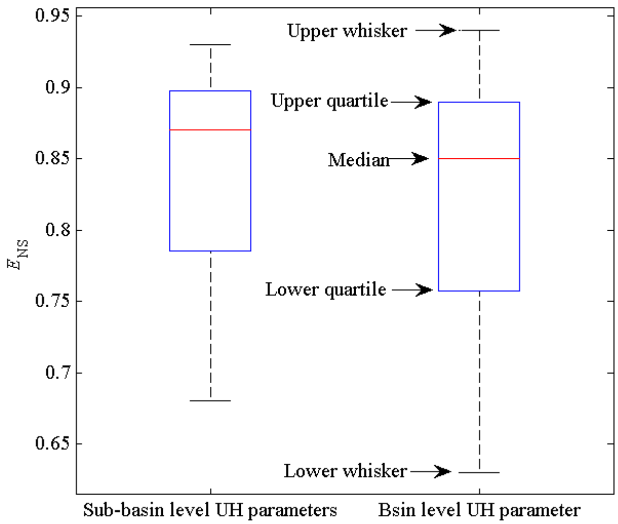

Figure 8 Box plots of E_{NS} values for the SWAT-EVENT model results for sub-basin level UH parameters and basin level UH parameters.

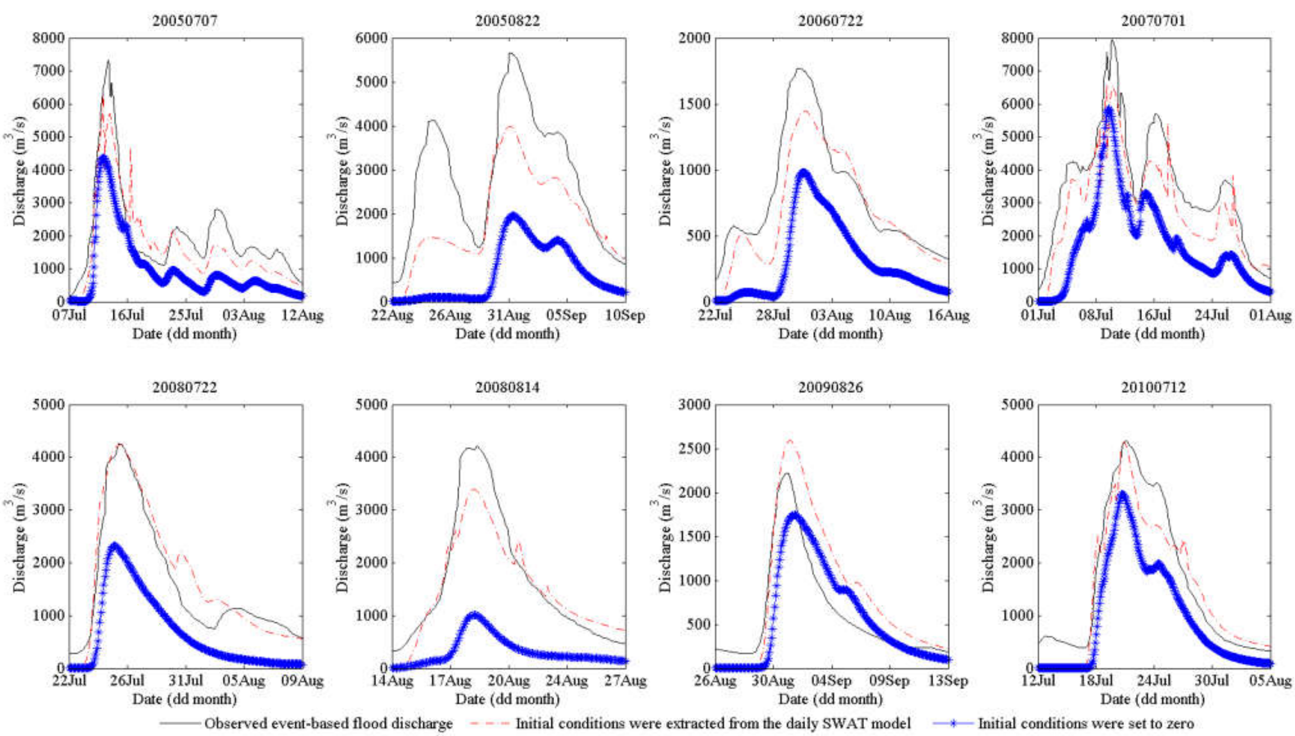

Figure 9 Impact of the antecedent conditions on the SWAT-EVENT model simulation results.